A physical explanation of excess quantum noise due to non-orthogonal modes

van der Lee, A.M.; van Exter, M.P.; van Druten, N.J.; Woerdman, J.P.

Publication date
2001

Published in
New Journal of Physics

New Journal of Physics
An Institute of Physics and Deutsche Physikalische Gesellschaft Journal

A physical explanation of excess quantum noise due to non-orthogonal modes

A M van der Lee, M P van Exter, N J van Druten† and J P Woerdman

Huygens Laboratory, Leiden University, PO Box 9504, Leiden, The Netherlands
E-mail: lee@molphys.leidenuniv.nl

New Journal of Physics **3** (2001) 2.1–2.15 (http://www.njp.org/)
Received 15 November 2000; online 23 March 2001

Abstract. We introduce a physical model of excess quantum noise in a laser with non-orthogonal polarization modes. We discuss the cause of the polarization excess quantum noise in terms of an injected wave excitation factor. Within this context the excess noise is due to the fact that the lasing mode is *not* the polarization state that experiences the highest gain.

1. Introduction

When first introduced by Klaus Petermann in 1979 for gain-guided lasers, the Petermann K-factor was controversial [1]. The K-factor (or excess noise factor) is the factor by which the quantum noise is enhanced with respect to the level set by the classical formula (of 1958) of Schawlow and Townes [2]. It was felt by some that since the Schawlow–Townes formula was set in the 'stone' of quantum mechanics, Petermann's result had to be in violation of fundamental principles. This controversy was later solved by Haus and Kawakami [3], who pointed out that the noise terms for different propagating modes in a loss- or gain-guided cavity are correlated and so were still in agreement with the fundamental principles of quantum mechanics.

In 1989 Siegman showed that the excess noise factor is not just a property of gain- or loss-guided lasers but of any laser cavity with non-orthogonal modes [4]. The loss of the laser cavity during a round trip makes the propagation of the light non-unitary, which can lead to non-orthogonal modes. However, the relationship between loss and non-orthogonality is a very subtle one. For different cavity configurations with the same average losses, the K-factor can have totally different values. The transverse eigenmodes of the most common laser resonator, the stable cavity, are also practically orthogonal and thus do not show an excess noise factor. This in contrast to an unstable resonator were non-orthogonal *transverse* eigenmodes appear naturally.

† Present address: Department of Applied Physics, Delft University of Technology, Lorentzweg 1, 2628 CJ Delft, The Netherlands.

PII: S1367-2630(01)19094-4

Experiments measuring the quantum-limited linewidth of such lasers have demonstrated large excess-noise factors [5, 6].

Our present interest is in non-orthogonal *polarization* modes. In a stable cavity with orthogonal transverse modes, one can make the polarization modes non-orthogonal; this gives a two-mode model system for studying excess quantum noise (in contrast to the many transverse modes in an unstable resonator). Large polarization K-factors have also been demonstrated experimentally [7, 8]. The polarization non-orthogonality has also proven to be a useful model system to demonstrate that excess quantum noise is coloured [9] and that excess quantum noise can seriously hinder intensity noise squeezing below the standard quantum limit [10]. In both situations, the transverse-mode case and the polarization-mode case, the excess noise factor is satisfactorily described by mode-non-orthogonality theory [4]. This theory formally connects non-orthogonal modes to excess noise, but it does not give a clear view on the physical origin of the excess noise factor.

For an unstable resonator a more physical picture of excess noise exists, in terms of the injected-wave excitation (*IWE*) factor [11]. In this picture the origin of excess quantum noise is attributed to the 'preamplification' of the quantum noise before it ends up in the lasing mode. A key role is played by the adjoint of the lasing mode, which is defined by the biorthogonality relation; it is the mode that is orthogonal to all other cavity eigenmodes (apart from the lasing mode). In a cavity with non-orthogonal transverse modes, a wave which has the same transverse mode profile as the adjoint mode excites the lasing mode most efficiently (even more efficient than the eigenmode itself). In an unfolded lens guide picture of an unstable resonator as depicted in figure 1, the physical reason of this excitation advantage is easily seen (this figure was taken from [12]). Before the adjoint mode ends up as the lasing mode it has a few loss-free round trips, whereas the eigenmode experiences loss each round trip due to its magnification. It has been shown that this excitation advantage is mathematically equivalent to the K-factor that follows from mode-non-orthogonality theory [4].

The purpose of this paper is to develop an analogous *IWE* picture for the non-orthogonal polarization modes, in order to clarify the physical origin of the excess quantum noise in this case. We can derive analytical results for the polarization dynamics, as the polarization state space consists of only two modes, contrary to the manifold of modes in transverse mode space. The article starts in section 2 with the basic equations that describe the polarization evolution and the separate polarization anisotropies, which together produce the non-orthogonal modes. Furthermore, we calculate the *IWE* factor for two distinct regimes in which the laser can operate; these regimes are the single-mode regime (section 3) and a peculiar two-mode regime (section 4). We end the article with conclusions (section 5).

2. Introducing the basic elements

In order to create non-orthogonal polarization modes one needs, in essence, two kinds of polarization anisotropies. The first is a polarization anisotropic loss and the second is a polarization anisotropic dispersion. When only one of the two is present the eigenmodes are orthogonal; only the mixture of the two can yield non-orthogonal modes.

Experimentally, two ways have been demonstrated to create non-orthogonal polarization modes. One is to use linear dichroism, i.e. a difference in loss of two orthogonal linear polarization states, in combination with circular birefringence, i.e. a difference in the refractive index of the $\sigma_{\pm}$ polarized states [7]. The other method is to use linear dichroism in

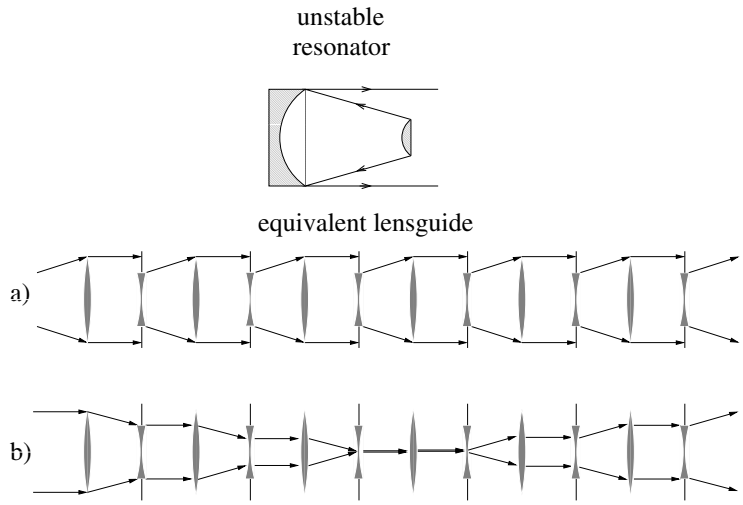

Figure 1. A confocal unstable resonator is depicted as a series of lenses that form a equivalent lens guide. A resonator round trip is then equivalent to moving one period through the lens guide. In (a) the eigenmode is depicted, in (b) the adjoint mode. In each round trip the eigenmode spills over the outcoupling mirror, whereas the adjoint mode is focused to its diffraction limit before it starts to diverge and becomes the eigenmode. So the adjoint mode has a number of loss-free round trips; this makes injection in this mode more efficient than injection in the eigenmode.

combination with (misaligned) linear birefringence, i.e. a difference in refractive index between two orthogonal linearly polarized states [8]. We have experimentally used the first method and this article will treat the polarization dynamics arising from a linear dichroism and a circular birefringence (see [7] for the experimental implementation of linear dichroism and circular birefringence).

We will model the laser as a linear amplifier with a fixed gain, the gain being equal to the losses. As the saturation is neglected this describes a laser at threshold. We choose the $\sigma_\pm$ states as a basis. The time evolution of the electric field is given by the following equation (see [13] for further discussion):

$$\frac{\mathrm{d}}{\mathrm{d}t}\begin{pmatrix} E_+ \\ E_- \end{pmatrix} = (M + gI)\begin{pmatrix} E_+ \\ E_- \end{pmatrix} \tag{1}$$

where E_+ and E_- are the (complex) amplitudes of the circular polarizations σ_+ and σ_-, respectively. The polarization evolution is separated into two parts. The (2×2) matrix M contains the polarization-anisotropic part of the evolution (the trace of M is zero). The real and imaginary parts of the eigenvalues of M determine the relative loss and the relative frequency of the eigenmodes respectively (where relative means, with respect to the loss and frequency of the modes in the absence of M). The isotropic part of the evolution is given by gI, where g is a constant and I is the unity matrix. The value of g is fixed by the condition that the lasing mode of the cavity has a net gain of zero. As the trace of M is zero, this implies that $g \leq 0$.

The dynamics of two complex mode amplitudes has, in principle, four degrees of freedom. As we are not interested in the overall phase factor, we are left with three remaining degrees of freedom which can be chosen as the intensity I and the two polarization parameters θ and χ,

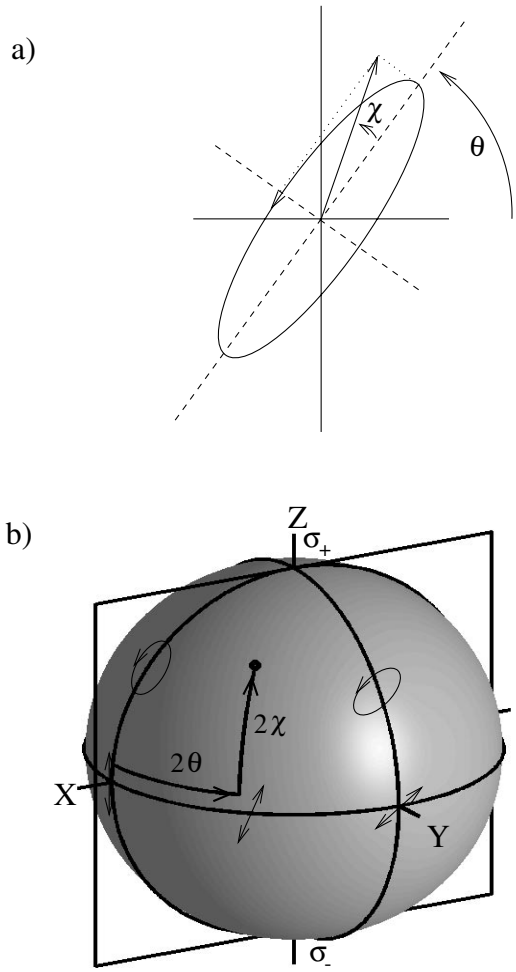

Figure 2. (a) The polarization ellipse which is characterized by two angles: θ, which gives the direction of the main axis of the ellipse, and χ, which characterizes its ellipticity. (b) The Poincaré sphere; a polarization state given by (θ, χ) is mapped to the point on the Poincaré sphere with azimuth 2θ and elevation 2χ. A few polarization states are shown on the sphere; at the equator the polarization is linear, at the poles it is circular and in between it is elliptical. The polarization dynamics on the surface of sphere is projected upon the plane through the X- and Z-axes indicated in the figure.

which characterize the direction of the main axis and the ellipticity angle of the polarization ellipse. To visualize the polarization state evolution we use the Poincaré sphere [14]. On the Poincaré sphere the polarization state (θ, χ) is characterized by a point with azimuth 2θ and elevation 2χ (see figure 2). So the poles correspond to $\sigma_{\pm}$ polarizations and the equator contains the linear polarizations. Note that orthogonal polarization states correspond to points that lie diametrically opposite on the sphere. The evolution of the polarization (θ, χ) can be represented by a trajectory on the surface of this Poincaré sphere (the intensity variation during the evolution is lost by projection on the surface of the sphere). In order to present the two-dimensional (2D) surface of the sphere onto the 2D plane of this paper, we make a projection of the front

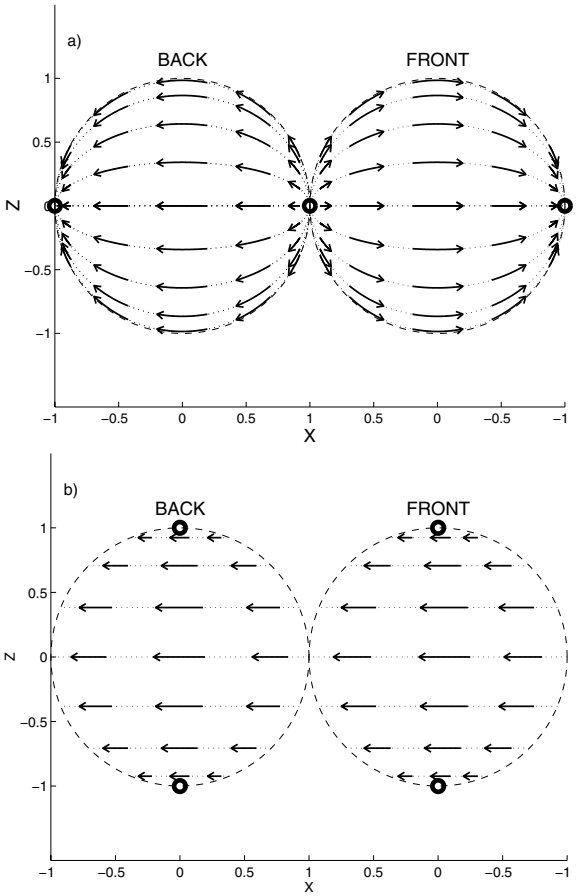

Figure 3. (a) Projection on the X–Z plane of the front and back side of the polarization flow pattern on the Poincaré sphere for the case of pure linear dichroism. The back side ($Y < 0$) is depicted on the left and the front side ($Y > 0$) is depicted on the right. The arrows along the flow lines indicate the direction of the evolution, while their length represents the rate of the evolution on the Poincaré sphere. The eigenmodes are indicated with a circle, **o**, the low-loss mode at $X = -1$ is linearly polarized with $\theta = \frac{1}{2}\pi$ and the high-loss mode is at $X = 1$ linearly polarized with $\theta = 0$. The flow lines point from the high-loss mode towards the low-loss mode. The eigenmodes are diametrically opposite on the sphere, indicating that the eigenmodes are orthogonal. (b) Projection to the X–Z plane of the front and back sides of the polarization flow pattern on the Poincaré sphere for the case of pure circular birefringence. The two stationary points are situated on the poles of the sphere and are indicated with a circle, **o**. The eigenmodes are the orthogonal $\sigma_{\pm}$ polarized states. The flow lines form circles around the eigenmodes parallel to the equator.

side ($Y > 0$) and back side ($Y < 0$) of the sphere onto a plane through the X and Z axes ($(X, Y, Z) \rightarrow (X, Z)$, see figure 3).

We first consider the properties of the two polarization anisotropies separately. In the case of linear dichroism with the high-loss axis in the direction $\theta = 0$, the matrix M in equation (1)

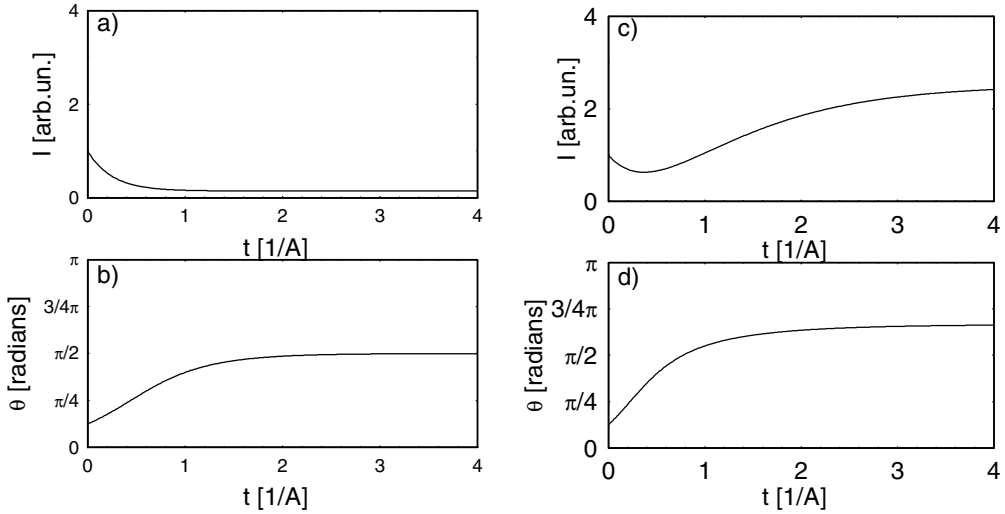

Figure 4. (a), (b) Typical evolutions of the intensity and polarization angle θ in the case of pure linear dichroism, where the eigenmodes are orthogonal. The starting polarization state is $\theta = \frac{1}{8}\pi$ and $\chi = 0$. (c), (d) Typical intensity and polarization angle evolutions for the situation where the linear dichroism dominates when the eigenmodes are non-orthogonal ($\Omega/A = \frac{1}{2}\sqrt{3}$, resulting in an excess noise factor of $K = 4$). The initial polarization state is again $\theta = \frac{1}{8}\pi$ and $\chi = 0$. Note that the final intensity is *larger* than its starting value in contrast to the case displayed in (a).

has the following form in the considered $\sigma_\pm$ basis:

$$M = \begin{pmatrix} 0 & -A \\ -A & 0 \end{pmatrix} \tag{2}$$

with $A > 0$. The polarization eigenmodes are aligned with the high-loss ($\theta = 0$, $\chi = 0$) and low-loss ($\theta = \frac{1}{2}\pi$, $\chi = 0$) axes of the linear dichroism. So they are orthogonal and linearly polarized, and have a difference in loss. In this case the value of g must be chosen as $-A$ so that the loss of the low-loss mode is zero and that of the high-loss mode is $2A$. Figure 3(a) shows the polarization dynamics on the Poincaré sphere by a flow line pattern, which indicates the polarization state evolution as described by equation (1). They point from the high-loss axis of the linear dichroism towards the low-loss axis, indicating the evolution of the polarization states towards the preferred axis as the high-loss component of the polarization damps out. The eigenmodes are identified as the source and sink points on the Poincaré sphere; the source point at $X = 1$ corresponds to the direction of high-loss and the sink point at $X = -1$ corresponds to the direction of low-loss.

In figures 4(a) and 4(b) we have plotted the evolution of the intensity and polarization angle for a starting polarization state with $\theta = \frac{1}{8}\pi$ and $\chi = 0$. This shows a 'typical' evolution of the polarization state. The polarization rotates towards the low-loss axis at $\theta = \frac{1}{2}\pi$. From the matrix description of equation (1) one finds that the intensity decreases monotonically towards a constant value as the high-loss polarization component of the initial polarization state decays, and the lasing mode component remains unchanged. The maximum power in the cavity is reached by injecting with the lasing eigenmode, in which case $I(t)$ becomes a constant.

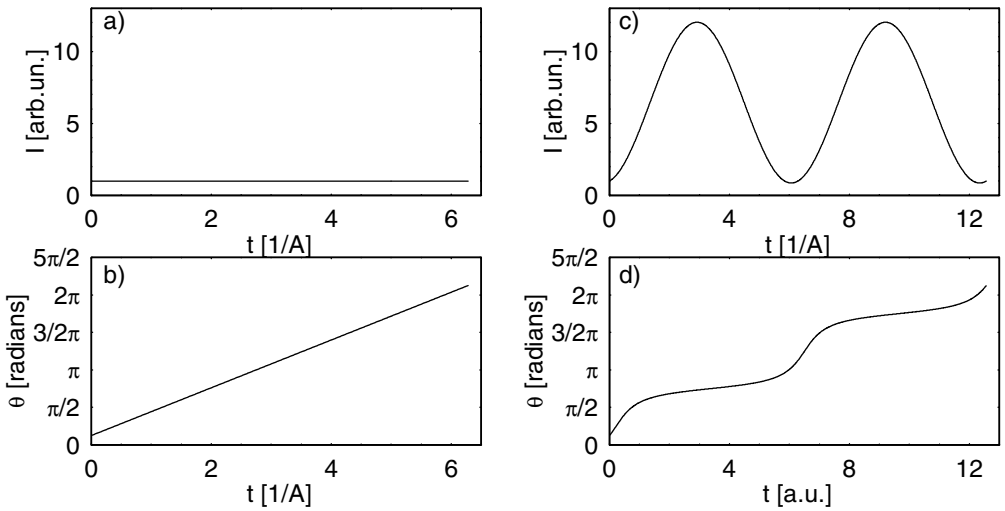

Figure 5. (a), (b) Typical evolutions of the intensity and polarization angle in the case of pure circular birefringence when the eigenmodes are orthogonal. The starting polarization state is $\theta = \frac{1}{8}\pi$ and $\chi = 0$. (c), (d) Typical evolutions of the intensity and polarization angle when circular birefringence dominates, but the eigenmodes are non-orthogonal ($\Omega/A = \frac{2}{3}\sqrt{3}$, resulting in $K = 4$). The initial polarization state is $\theta = \frac{1}{8}\pi$ and $\chi = 0$. Note that the intensity is modulated, and has an average power which is *larger* than one, in contrast to the intensity evolution displayed in (a) where the intensity remains constant at a value of one.

We now address the circular birefringence, which is represented by the following matrix M:

$$M = \begin{pmatrix} \mathrm{i}\Omega & 0 \\ 0 & -\mathrm{i}\Omega \end{pmatrix} \tag{3}$$

with $\Omega > 0$. This matrix is diagonal, so the eigenmodes and eigenvalues are easily identified as the orthogonal $\sigma_{\pm}$ polarization states having different frequencies. The circular birefringence is a dispersive anisotropy whereas the linear dichroism is an absorptive anisotropy. This difference appears in the flow line pattern on the Poincaré sphere (compare figures 3(a) and 3(b)); in the dispersive case the polarization evolution corresponds to a constant angular velocity along a trajectory parallel to the equator of the sphere. In figures 5(a) and 5(b), an example for the evolution of the polarization angle and the intensity is shown with, as starting values, $\theta = \frac{1}{8}\pi$ and $\chi = 0$. The polarization rotates at constant speed and the intensity remains constant. As there is no loss difference between the orthogonal eigenmodes, the intensity remains constant for any starting polarization state, hence all the polarization states couple equally efficiently to the laser cavity.

To make the eigenmodes non-orthogonal we need both anisotropies together; this gives the following matrix M:

$$M = \begin{pmatrix} \mathrm{i}\Omega & -A \\ -A & -\mathrm{i}\Omega \end{pmatrix}. \tag{4}$$

The eigenvalues of this matrix are $\lambda = \pm\sqrt{A^2 - \Omega^2}$, which are either real or imaginary depending on the relative strength of the anisotropies $|\Omega|/A$. This yields two distinct regimes, which

we will first briefly introduce (a more detailed discussion is given in sections 3 and 4). A graphical representation of the loss difference, frequency difference and polarization state of the eigenmodes is found in figure 1 of [7].

In the first regime ($|\Omega| < A$) the linear dichroism dominates. The eigenmodes are linearly polarized and have a difference in loss, but the same frequency. The polarization eigenmodes become non-orthogonal as soon as $\Omega \neq 0$. In this situation the laser will be single mode as the gain only compensates the losses of the low-loss mode. In analogy to a ring-laser gyro [15] we will call this the locked regime, as both eigenmodes have the same frequency. Single-mode operation is the usual situation for a laser with excess noise, therefore the *IWE* picture will show many similarities to that of an unstable resonator.

In the second regime ($|\Omega|/A > 1$) the circular birefringence dominates. The eigenmodes are then elliptically polarized and have the same loss but a different frequency. The polarization modes become non-orthogonal as soon as $A \neq 0$. In this situation both eigenmodes will lase and we have a two-mode laser. In analogy to a ring-laser gyro we will call this situation the unlocked regime. This is a multi-mode laser with non-orthogonal eigenmodes, an unusual but interesting situation. The corresponding *IWE* factor will demonstrate different behaviour from that of an unstable resonator.

As an aside we compare the discussion given above with the other case where polarization-mode non-orthogonality has been realized, based upon combining linear birefringence and linear dichroism [8]. If we assume that the axis of the linear birefringence is at $45°$ with respect to the linear dichroism, we find the same matrices as given above when we change the basis from the $\sigma_\pm$ states to the x, y linearly polarized states (with x, y along the main axis of the linear birefringence). The appropriate polarization states are obtained by performing a rotation of the Poincaré sphere over $90°$ around the Z-axis followed by a rotation over $90°$ around the Y-axis.

3. The locked regime

We start by describing the locked regime, where the linear dichroism is dominant ($|\Omega| < A$). The resulting flow pattern is a superposition of the flow patterns for the case of pure linear dichroism and pure circular birefringence (see figure 3); it is displayed in figure 6. The ratio of the strength of the two anisotropies has been chosen as $\Omega/A = \frac{1}{2}\sqrt{3}$. This pattern is similar to the flow pattern of pure dichroism (figure 3(a)) in the sense that it contains two stationary points which are a source and a sink for the flow lines. The important difference, however, is that the stationary points are no longer diametrically opposite, i.e. the eigenmodes are non-orthogonal. This demonstrates that we need both an absorptive and a dispersive anisotropy to create non-orthogonal modes. The major consequence of the non-orthogonality of the modes is that the low-loss axis of the linear dichroism, which is at $X = -1$, is no longer aligned with the lasing eigenmode, which is at $X = -0.5$ at the back side of the projection plane. As the gain of the laser medium is equal to the loss of the lasing eigenmode, there is net gain in the region on the Poincaré sphere where the losses are less than that of the low-loss eigenmode. In figure 6 this net gain region is indicated in grey. This region is divided into three sub zones to schematically show the increase in gain when approaching $X = -1$. This net-gain region has the low-loss direction of the linear dichroism ($X = -1$) as its centre.

Figures 4(c) and 4(d) readily shows the consequence of this in a 'typical' evolution of I, θ starting from the polarization state ($\theta = \frac{1}{8}\pi$, $\chi = 0$). The evolution of the polarization angle is still similar to that for the case of pure dichroism. However, the intensity evolution is radically

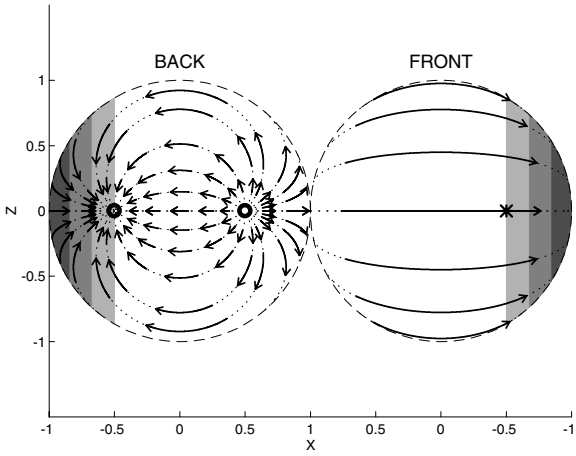

Figure 6. Polarization state evolution in the case when the ratio of linear dichroism and circular birefringence is $\Omega/A = \frac{1}{2}\sqrt{3}$, represented on a Poincaré sphere. The stationary points (indicated with a circle, **o**) correspond to the eigenmodes, the flow lines point from the high-loss eigenmode to the low-loss eigenmode. The flow pattern looks significantly different on the back and front sides of the Poincaré sphere as a consequence of the non-orthogonal eigenmodes. Because the low-loss axis of the linear dichroism is no longer the same polarization state as the low-loss eigenmode (compare with figure 3(a)), a region of net gain exists on the Poincaré sphere. The grey scale in the figure indicates this net-gain region (the blacker the region, the higher the gain). The adjoint mode $|a_1\rangle$ is indicated with an asterisk, $*$.

different. When the polarization state reaches the region on the Poincaré sphere where the loss is less than that of the lasing eigenmode ($\frac{1}{3}\pi < \theta < \frac{2}{3}\pi$), the intensity rises, and actually exceeds the starting value. This is a counterintuitive property of any laser with non-orthogonal modes: the lasing eigenmode is no longer the mode with the lowest loss.

We quantify now this qualitative picture of feeding the laser with an arbitrary polarization state. First we derive the eigenvalues, eigenmodes, and the adjoint modes of $M + gI$ (with M as in equation (4)). Then we use the eigenmodes and adjoint modes to calculate, via mode-non-orthogonality theory, the excess-noise factor. After that we will calculate the key quantity of this paper, namely the *IWE* factor for an arbitrary polarization state, i.e. we calculate the ratio of the final power ending up in the lasing mode and the starting power. We can use the *IWE* factor to find which polarization state couples most efficiently to the lasing mode. Also, we average the *IWE* factor over all polarization states and compare this with the result in the case of orthogonal eigenmodes. This ratio gives the (average) preamplification factor of the quantum noise.

We start by calculating the eigenvalues λ_i of $M+gI$, choosing the value of $g = -\sqrt{A^2 - \Omega^2}$, this yields

$$\lambda_1 = 0 \tag{5}$$

$$\lambda_2 = -2\sqrt{A^2 - \Omega^2} \tag{6}$$

where the index 1 corresponds to the lasing eigenmode and the index 2 to the non-lasing

eigenmode. The corresponding eigenvectors in the usual $\sigma_\pm$ basis are

$$|e_1\rangle = \frac{1}{\sqrt{2}}\begin{pmatrix} 1 \\ \mathrm{e}^{2\mathrm{i}(\pi/4+\phi)} \end{pmatrix} \qquad |e_2\rangle = \frac{1}{\sqrt{2}}\begin{pmatrix} 1 \\ \mathrm{e}^{2\mathrm{i}(\pi/4-\phi)} \end{pmatrix} \tag{7}$$

where $\cos 2\phi = \Omega/A$, $0 \leq \phi \leq \pi/2$. From equation (7), we deduce that the eigenmodes are linearly polarized ($|E_+| = |E_-|$) and the polarization angle θ is $-\pi/4 - \phi$ for the low-loss mode $|e_1\rangle$ and $-\pi/4 + \phi$ for the high-loss eigenmode $|e_2\rangle$. The biorthogonality relation ($\langle a_i|e_j\rangle = \delta_{ij}$) is used to determine the corresponding adjoint modes $|a_1\rangle, |a_2\rangle$:

$$|a_1\rangle = \frac{1}{\sqrt{2}}\begin{pmatrix} 1 \\ \mathrm{e}^{-2\mathrm{i}(\pi/4+\phi)} \end{pmatrix} \qquad |a_2\rangle = \frac{1}{\sqrt{2}}\begin{pmatrix} 1 \\ \mathrm{e}^{-2\mathrm{i}(\pi/4-\phi)} \end{pmatrix} \tag{8}$$

which are again normalized. These adjoint modes are also linearly polarized but their polarization angles differ namely, $\pi/4 + \phi$ for $|a_1\rangle$ and $\pi/4 - \phi$ for $|a_2\rangle$.

Knowing both eigenmodes and adjoint modes we calculate the expected excess-noise factor, using the well known recipe [4]:

$$K = \frac{\langle e_1|e_1\rangle\langle a_1|a_1\rangle}{|\langle a_1|e_1\rangle|^2} = \frac{1}{\sin^2 2\phi} = \frac{1}{1-(\Omega/A)^2}. \tag{9}$$

Note the straightforward relation between the enhancement factor and the polarization angle difference of 2ϕ.

We now address the *IWE* factor of an arbitrary polarization state. With the eigenmodes and eigenvalues of $M + gI$ we can calculate the final intensity in the lasing mode from equation (1). For this calculation we transform an arbitrary normalized polarization state from the $\sigma_\pm$ basis to the non-orthogonal eigenbasis (equation (7)), and determine the amplitude of the lasing mode component, E_1. The non-lasing mode component is negligible after a sufficiently long time as it experiences a net loss. The square of the amplitude of E_1 yields the following *IWE* factor:

$$IWE = I(t \to \infty) = |E_1|^2 = \frac{K}{2}[1 - \cos(2\chi)\sin(2\phi - 2\theta)] \tag{10}$$

for injection with a polarization state given by a polarization angle θ and ellipticity χ. Substituting the eigenmodes into equation (10) gives the expected results. We find $IWE = 1$ for injection with the lasing eigenmode and the $IWE = 0$ for injection with the non-lasing eigenmode. The maximum of equation (10) occurs when the light is linearly polarized ($\chi = 0$) at a polarization angle $\theta = \pi/4 + \phi$. This polarization state is equal to the adjoint mode $|a_1\rangle$.

The preamplification of the quantum noise is calculated by averaging the *IWE* factor over all possible injection states for the case of non-orthogonal modes and for orthogonal modes ($K = 1$):

$$\frac{\langle IWE_K\rangle}{\langle IWE_{K=1}\rangle} = \frac{(K/2)\langle[1 - \cos(2\chi)\sin(2\phi - 2\theta)]\rangle}{(1/2)\langle[1 - \cos(2\chi)\sin(\pi/2 - 2\theta)]\rangle} = K \tag{11}$$

where $\langle\cdots\rangle$ means averaging over all polarization states. The terms in the numerator and denominator containing $\sin 2\theta$ average out to zero. Thus equation (11) shows that the preamplification of the quantum noise is equal to the excess noise factor following from mode-non-orthogonality theory.

Why is the adjoint mode maximally efficient in exciting the laser mode? This is readily seen in figure 6. The adjoint mode $|a_1\rangle$ (indicated with an asterisk, $*$) is positioned just at the border of the net-gain region. During evolution the polarization state moves towards the lasing eigenmode and spends all of its time in the net gain regime, where it profits maximally from

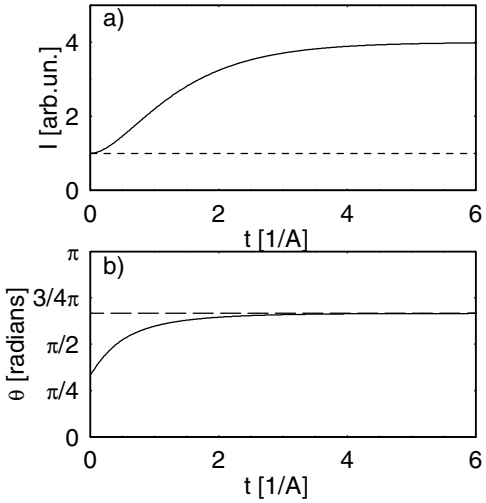

Figure 7. (a) Evolution of the intensity in the laser with $K = 4$ when starting in the adjoint mode (full curve) or eigenmode (broken line). (b) Corresponding evolution of the polarization angle. This figure clearly demonstrated the power advantage of injecting the laser cavity with the adjoint mode instead of the usual eigenmode.

the net gain. In analogy with the unstable resonator, it experiences, in the beginning, less loss than the lasing mode. The polarization angle and intensity evolution of the adjoint mode and eigenmode are plotted in figure 7. The polarization of the adjoint modes rotates towards the eigenmode and the final intensity is K times as much as the unit power with which it started (for $\Omega/A = \frac{1}{2}\sqrt{3}$, $K = 4$). This clearly demonstrates the excitation advantage of the adjoint mode over excitation in the eigenmode. Note that the build-up time of this excess power corresponds to the decay time of the non-lasing polarization mode, which is in our experiment typically 100 cavity round trips (a polarization anisotropic loss of 1% of the total cavity losses, and the total cavity losses are roughly 70% per round trip, see [7]). This is much slower than in an unstable resonator where it is typical a few round trips (see figure 1 and [12]).

4. The unlocked regime

To describe the situation where circular birefringence dominates ($|\Omega| > A$), we start with the pure circular-birefringence flow pattern and add a bit of the linear-dichroism flow pattern. This results in the flow pattern of figure 8. This flow pattern is similar to that of pure circular birefringence (cf figure 3(b)) in the sense that the polarization flow lines form closed loops around the eigenmodes. This corresponds to the fact that in this case the eigenmodes have a frequency difference but no loss difference. The laser operates in the two eigenmodes simultaneously, thus distinguishing this situation from the single-mode laser usually considered in excess-noise theory. The main difference in the flow pattern compared to the case of pure circular birefringence is that the stationary points will no longer be at the poles, but on the meridian through $X = 0$, at the points where the flow of the linear dichroism to the right is compensated by the flow of the circular birefringence to the left (see figure 3). These points are no longer diametrically opposite on the Poincaré sphere, so that they correspond to non-orthogonal eigenmodes. Again there

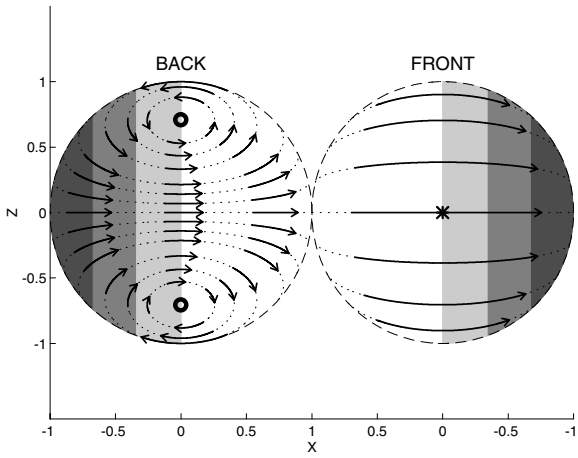

Figure 8. Flow pattern on the Poincaré sphere when the circular birefringence dominates over the linear dichroism ($\Omega/A = \frac{2}{3}\sqrt{3}$). The flow lines are all closed loops around the eigenmodes, but in contrast to the case of pure circular birefringence the stationary points are no longer on the poles, the eigenmodes (indicated with a circle, **o**) are non-orthogonal. The grey region indicates the net-gain region, it is subdivided into three zones. The blacker the region, the higher is the gain. The polarization state which injects the most power into laser is indicated with an asterisk, $*$.

is a net-gain region on the Poincaré sphere. The presence of the linear dichroism leads to a polarization dependence of the loss; for $X < 0$ the loss is less than that of the eigenmodes and results in a net gain, for $X > 0$ the loss is more than that of the eigenmodes and results in a net loss. In figure 8 the net-gain region is indicated with a grey scale (the blacker, the higher the gain).

Figure 5(c) and 5(d) depicts a 'typical' evolution of the intensity and polarization angle. The starting point is linearly polarized light with $\theta = \frac{1}{8}\pi$ and $\chi = 0$. In this figure the differences with pure circular birefringence (figures 5(a) and 5(b)) are easily seen: the intensity is oscillating instead of constant and the polarization no longer rotates with a constant angular speed. The modulation of the intensity is caused by the passage of the polarization state through the net-gain and net-loss regions on the Poincaré sphere. One also notices that the average gain of the polarization state is zero as the intensity comes back to unity after each cycle. The mean power during the round trip on the Poincaré sphere, however, is larger than in the case of pure circular dichroism (cf figure 5(a)). Again, excitation with the eigenmode is no longer the most efficient way to inject power into the laser cavity.

We will now quantify this qualitative picture of feeding the laser by an arbitrary polarization state. For the considered two-mode laser in the unlocked regime we will calculate the *IWE* factor, thus evaluating the effect of injecting light with an arbitrary polarization state. As the laser intensity generally oscillates we define the *IWE* factor as the average power of a cycle normalized to its starting power at injection. We can use the *IWE* factor to find which polarization state couples most efficiently into the laser. To calculate the preamplification factor of the quantum noise we take the ratio of the *IWE* averaged over all polarization states for non-orthogonal modes and for orthogonal modes.

The dynamics of the polarization state evolution is governed by the eigenvalues and eigenmodes of $M + gI$. The value of g is chosen as zero. The eigenvalues are

$$\lambda_1 = \mathrm{i}\sqrt{\Omega^2 - A^2} \tag{12}$$

$$\lambda_2 = -\mathrm{i}\sqrt{\Omega^2 - A^2}. \tag{13}$$

They yield a difference in frequency and zero net loss. The corresponding eigenmodes are

$$|e_1\rangle = \begin{pmatrix} \cos(\zeta - \pi/4) \\ \mathrm{i}|\sin(\zeta - \pi/4)| \end{pmatrix} \qquad |e_2\rangle = \begin{pmatrix} |\sin(\zeta - \pi/4)| \\ \mathrm{i}\cos(\zeta - \pi/4) \end{pmatrix} \tag{14}$$

with $\cos 2\zeta = (A/\Omega)$ and $0 \leq \zeta \leq \pi/2$. The angle ζ corresponds to the ellipticity of the eigenmodes. The eigenmodes are elliptically polarized with opposite helicity, and their polarization angle θ is $-\frac{1}{4}\pi$ (radians). The adjoint modes are the polarization states that are rotated by 180° on the Poincaré sphere and have the same ellipticity as the corresponding eigenmode:

$$|a_1\rangle = \begin{pmatrix} \cos(\zeta - \pi/4) \\ -\mathrm{i}|\sin(\zeta - \pi/4)| \end{pmatrix} \qquad |a_2\rangle = \begin{pmatrix} |\sin(\zeta - \pi/4)| \\ -\mathrm{i}\cos(\zeta - \pi/4) \end{pmatrix}. \tag{15}$$

Use of the mode-non-orthogonality theory yields an excess noise factor of

$$K = \frac{1}{\sin^2 2\zeta} = \frac{1}{1 - (A/\Omega)^2}. \tag{16}$$

To calculate the intensity evolution we first transform a normalized polarization state in the $\sigma_\pm$ basis to the eigenbasis to calculate the evolution of its components; subsequently we transform it back to the orthogonal $\sigma_\pm$ basis to calculate its intensity. This yields

$$I(t) = |E_1|^2 + |E_2|^2 + 2\sqrt{1 - \frac{1}{K}}\,\mathrm{Re}[E_1 E_2^*\,\mathrm{e}^{2\mathrm{i}\sqrt{\Omega^2 - A^2}t}] \tag{17}$$

$$|E_1|^2 + |E_2|^2 = K\left[1 + \cos(2\chi)\sin(2\theta)\sqrt{1 - \frac{1}{K}}\right] \tag{18}$$

and

$$2E_1E_2^* = -K\left[\sqrt{1 - \frac{1}{K}} + \cos(2\chi)\sin(2\theta) - \mathrm{i}\sqrt{\frac{1}{K}}\cos(2\chi)\cos(2\theta)\right] \tag{19}$$

for an arbitrary polarization state characterized by (θ, χ). We introduced E_1 and E_2 as the amplitudes of the non-orthogonal eigenmodes. Equation (17) gives the intensity evolution $I(t)$, which has an oscillatory behaviour. The average value of the intensity is given in equation (18), the amplitude of the oscillation in equation (19). Equations (17)–(19) yield the expected result for injection with the polarization eigenmodes, namely a constant value $I(t) = 1$.

The *IWE* factor of a given polarization state is given by the mean power in the cavity, equation (18). The maximum average power is realized when we inject a polarization state with $\theta = \frac{1}{4}\pi$ and $\chi = 0$. This leads to $IWE = K + \sqrt{K(K-1)}$. Note that this polarization state does not correspond with one adjoint mode, as it always does for a single-mode laser, and that its *IWE* is *larger* than K. This polarization state is actually a superposition of both adjoint modes $|x\rangle = (|a_1\rangle + |a_2\rangle)/\sqrt{2}$. As both eigenmodes lase simultaneously it is no longer a question of exciting one eigenmode maximally by injecting with a adjoint mode, but instead to excite both eigenmodes together maximally.

As above, the physical reason why injection via this superposition of the two adjoint modes excites the cavity maximally is easily seen on the Poincaré sphere. This polarization state is a

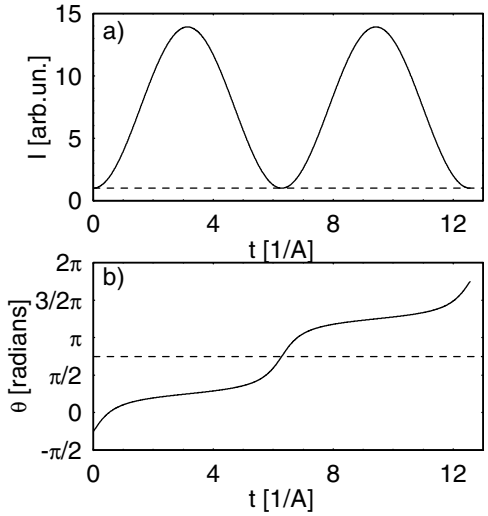

Figure 9. (a) Evolution of the intensity in the laser with $K = 4$ when starting in the superposition of the adjoint mode that leads to optimal injection (full curve) or in the eigenmode (dashed line). (b) Corresponding evolution of the polarization angle. Note that the average intensity of injection with the adjoint mode is substantially higher than with the eigenmode.

point on the equator just at the border of the net-gain regime (indicated with an asterisk, $*$, in figure 8). The intensity and polarization angle evolution of this polarization state is depicted in figure 9. This evolution profits most from the net-gain regime. For the whole first-half of its cycle it experiences gain, thus its power only rises. Also, it passes over the low-loss axis of the dichroism, which is the point where the net gain is the largest ($X = -1$). For the second-half of its cycle it passes through the region of net loss and decays back to its original excitation. Its average power is clearly larger than unity.

By calculating the polarization averaged *IWE* for non-orthogonal and orthogonal modes, we obtain the enhanced noise power in the laser for random noise:

$$\frac{\langle IWE_K\rangle}{\langle IWE_{K=1}\rangle} = \frac{K\langle 1+\cos(2\chi)\sin(2\theta)\sqrt{1-(1/K)}\rangle}{\langle 1\rangle} = K \tag{20}$$

where $\langle\cdots\rangle$ indicates averaging over all polarization states, the averaging of the term with $\sin 2\theta$ gives zero, and we substituted $K = 1$ in equation (18) in the *IWE* factor for orthogonal modes. Although the polarization dynamics in this two-mode lasing regime is completely different from that of a single-mode laser, the K-factor derived from mode-non-orthogonality theory is still equal to the preamplification factor of the quantum noise.

5. Conclusions

In conclusion, a laser with non-orthogonal polarization modes is an ideal model system for studying excess quantum noise. As it contains only two polarization modes, it is much simpler than an unstable resonator with many transverse modes. The simplicity of the system makes it possible to calculate its polarization dynamics analytically. We have investigated a laser cavity

with a linear dichroism in combination with a circular birefringence, for which we have derived the *IWE* picture. In the locked regime the laser is single mode and we found the expected result that adjoint mode injection is the most advantageous injecting power into the lasing mode. The physics of this excitation advantage lies in the existence of a net-gain region on the Poincaré sphere. This net-gain region arises as the low-loss axis of the dichroism is not aligned with the direction of the eigenmode.

In the unlocked regime of the two polarization modes we have the peculiar case of a two-mode laser. The excess noise is still present, but in contrast to the single-mode laser, where the intensity in the lasing mode reaches a stationary value after the non-lasing mode has decayed, the intensity of the laser is oscillating with the beat frequency of the eigenmodes. Although the intensity returns to its initial value after each round trip on the Poincaré sphere, its average power during a cycle can be much larger than the original excitation. This is again caused by a region of net gain on the Poincaré sphere. By averaging over all polarization states of *IWE*, we again find a preamplification of the quantum noise due to non-orthogonal modes, which is equal to K.

Acknowledgments

We would like to acknowledge support of the Stichting voor Fundamenteel Onderzoek der Materie (FOM) which is supported by NWO, and from the European Union under TMR contract No ERB4061PL95-1021 (Microlasers and Cavity QED). The research of N J van Druten was made possible by the 'Koninklijke Nederlandse Akademie van Wetenschappen'.

References

[1] Petermann K 1979 *IEEE J. Quantum Electron.* **15** 566
[2] Schawlow A L and Townes C H 1958 *Phys. Rev.* **112** 1940
[3] Haus H and Kawakami S 1985 *IEEE J. Quantum Electron.* **21** 63
[4] Siegman A E 1989 *Phys. Rev.* A **39** 1253
Siegman A E 1989 *Phys. Rev.* A **39** 1264
[5] Cheng Y-J, Fanning C G and Siegman A E 1996 *Phys. Rev. Lett.* **77** 627
[6] van Eijkelenborg M A, Lindberg Å M, Thijssen M S and Woerdman J P 1996 *Phys. Rev. Lett.* **77** 4314
[7] van der Lee A M *et al* 1997 *Phys. Rev. Lett.* **79** 4357
[8] Emile O, Brunel M, le Floch A and Bretenaker F 1998 *Europhys. Lett.* **43** 153
[9] van der Lee A M *et al* 1998 *Phys. Rev. Lett.* **81** 5121
[10] van der Lee A M *et al* 2000 *Phys. Rev. Lett.* **85** 4711
[11] New G H C 1995 *J. Mod. Opt.* **42** 799
[12] van Eijkelenborg M A, Lindberg Å M, Thijssen M S and Woerdman J P 1997 *Phys. Rev.* A **55** 4556
[13] van der Lee A M *et al* 2000 *Phys. Rev.* A **61** 033812
[14] Born M and Wolf E 1998 *Principles of Optics* 6th edn (Cambridge: Cambridge University Press)
[15] Chow W W *et al* 1985 *Rev. Mod. Phys.* **57** 61